Vol 6 Issue 10 July 2017
ISSN No : 2249-894X

Monthly Multidisciplinary Research Journal

Review Of Research Journal

Chief Editors

Ashok Yakkaldevi
A R Burla College, India

Ecaterina Patrascu
Spiru Haret University, Bucharest

Kamani Perera
Regional Centre For Strategic Studies, Sri Lanka

Welcome to Review Of Research

RNI MAHMUL/2011/38595 **ISSN No.2249-894X**

Review Of Research Journal is a multidisciplinary research journal, published monthly in English, Hindi & Marathi Language. All research papers submitted to the journal will be double - blind peer reviewed referred by members of the editorial Board readers will include investigator in universities, research institutes government and industry with research interest in the general subjects.

Address:-Ashok Yakkaldevi 258/34, Raviwar Peth, Solapur - 413 005 Maharashtra, India
Cell : 9595 359 435, Ph No: 02172372010 Email: ayisrj@yahoo.in Website: http://oldror.lbp.world/

REVIEW OF RESEARCH

ISSN: 2249-894X
IMPACT FACTOR : 3.8014(UIF)
VOLUME - 6 | ISSUE - 10 | JULY - 2017

OPTIMIZATION OF GROUND PENETRATING RADAR (GPR) DATA INTERPRETATION FROM HYDROCARBON CONTAMINATION ON SUBSURFACE

Jamile Dehaini[1] , **Fábio Taioli**[2] ,**Jorge Kazuo Yamamoto**[3] ,
Antonio Claudio Kieling[4] ,**Jaidete Monteiro de Souza**[5] ,
Melquizedec Arcos Rodrigues[6] ,**Marcos Dantas dos Santos**[7]
[1]PhD in Geosciences, professor and researcher at Amazonas State University - UEA.
[2, 3]PhD in Geosciences, professors and researchers at São Paulo State University - USP.
[5]PhD in Meteorology, professor and researcher at Amazonas State University - UEA.
[4,6,7]Professors and researchers at Amazonas State University - UEA.

ABSTRACT

Leakage from gas stations, the refineries and pipelines is a common source of underground pollution and the subject has called attention of the academic, environmental and general community. Sometimes the leakage is followed by explosion and fire risks besides the inherent danger to the human health. Hydrogeologic and hydrogeochemical studies have shown that the hydrocarbon dispersion and migration mechanisms are complex and the adequate estimation is very difficult using solely monitoring wells. The application of indirect (geophysical) methods becomes even more complicated when occurring in an urban area where electrical, electromagnetic, seismic and other cultural noises are present and the data interpretation is very dependent of the geophysicist judgment. In order to make the ground penetrating radar (GPR) data interpretation more impersonal, an algorithm based on the amplitude spectra ratio was suggested and tested in a set of real data. The algorithm consists in the ratio between the maximum amplitude of the spectrum of the entire survey line and the maximum amplitude of parts of the spectrum, both in time and position. A geostatistical analysis of the results of the several calculated ratios was carried out and a new map was generated. The contamination, first visually characterized by a "shadow zone" in the GPR sections, was precisely detected using the suggested algorithm. After the drilling of boreholes in both contaminated and non-contaminated areas, chemical analysis of the water present in such boreholes confirmed the interpretation of the GPR sections and the precise extension of the contaminant plume obtained by using the algorithm., larger than previously estimated by the direct investigation and by the GPR visual interpretation.

INTRODUCTION

Groundwater hydrocarbon contamination case studies have been successfully carried out by using GPR (Benson, 1995; Daniels et al., 1995; Benson et al., 1997; Bermejo et al., 1997; Nash et al., 1997; Nguyen et al., 1997; Sauck et al., 1998, Lane et al., 2000, Dehaini, 2001). Otherwise, the reason that causes the visual effect on the GPR data is unknown and very controversial. Sauck et al., 1998 show that the knowledge on electromagnetic behavior of hydrocarbon contaminants in subsurface is incipient and must be studied.

In general, the case histories presented in the technical literature deal with controlled experiments where the GPR signal is analyzed before and after the contamination and in favorable environments for the propagation of the GPR pulse (sandy lithology, thick hydrocarbon free phase layer and sites with very low cultural noise).

Conversely, the real case is very different of the idealized experimental conditions. The most important source of hydrocarbon contamination in the soil and groundwater is the leakage of storage tanks in gas stations. Normally, gas stations are located in urbanized areas where electrical, electromagnetic, seismic and other types of cultural noises are present. In addition, it is common, mainly in tropical environment, the presence of a shallow clayey sediment layer that makes the application and data interpretation of GPR very difficult, because its relatively high conductance.

São Paulo city is one of the most urbanized and populated cities in the world, with gas stations spread all over. The hydrocarbon storage tanks of the gas stations are about 15 years old (Pacheco, 2000) and without any kind of environmental protection. Whenever a leakage happens, the health and explosion risk situation pushes to a rapid solution in order to decrease the risks to the neighbor population. Therefore the application of GPR to directly detect hydrocarbon in São Paulo is not common since whenever its presence is noted, a remediation process is installed and several boreholes are made to rapidly pump the contaminant and, consequently, to decrease the risk of an accident. After the extraction of the free phase, the vapor and residual phases stay being a permanent source of contamination to the groundwater and very difficult to be mapped and delimited only by boreholes and monitoring wells.

Under such scenario, the main objective of this research was to develop a mathematical treatment of the GPR data to rapidly determine the extent of the contamination plume avoiding, as much as possible, the subjectivity imposed by the conventional data interpretation.

BIBLIOGRAPHY REVIEW

It is well known that geoelectric are the most efficient and economical methods to study groundwater behavior through contrasts of the electric resistivity (or its inverse, electric conductivity), the dielectric constant and the magnetic permeability (Keller and Frischnecht, 1966; Orellana, 1982; Telford et al., 1990).

The electromagnetic properties of geologic materials are controlled primarily by its water content (Topp et al., 1980). Normally, the natural water present in the environment has appreciable electrical conductivity since brings a variable concentration of dissolved salts. The soil and rocks have pores or fractures that can be totally or partially filled with electrolite, that gives an ionic character with very variable resistivity (Orellana, 1982). The dielectric constant of the water is another electromagnetic property that can generate contrast with other materials in the medium (Topp et al., 1980).

The variation of the electromagnetic properties of the soil is generally associated with those differences that, in turn, cause reflections and attenuation of the GPR signal. The reflected signal is detected by the receiver antennae, amplified, digitized and recorded in a magnetic media for later processing and display of the data (Davis and Annan, 1989).

GPR data are normally presented in a section showing the two way traveltime (in ns) versus position measured at the surface. If the electromagnetic pulse velocity is known, the reflector depth can be calculated as (Benson, 1995):

$$z \cong \frac{vt_r}{2} \qquad \text{equation 1}$$

where z is the reflector depth, tr is approximately the two way time of the signal and v is the velocity that the signal travels in the underground material.

For low loss uniform medium with relative dielectric constant known (or estimated) K', one can replace v into the equation 1 and the depth of the reflector is given by (Benson, 1995):

$$z = \frac{ct_r}{2\sqrt{K'}} \qquad \text{equation 2}$$

where c is the speed of light in vaccum.

The penetration capacity of the GPR systems depends on the equipment power, central frequency and characteristics of the antennae, and electromagnetic properties of the underground materials (resistivity and permitivity). The amplitude of the GPR signal decreases as it propagates through the ground due to geometric divergence, partial transmission, reflection in the interfaces, scattering from thin layers and absorption of energy in the medium. The attenuation, or loss of the signal is caused by energy conversion to heat due to the electric conduction, loss by dielectric relaxation of the water molecules and/or chemical diffusion in clay minerals. Therefore, materials with high conductivity (e.g. clayey soils) can quickly reduce the signal depth penetration.

The relative permitivity, or dielectric constant, of each underground material or substance is the factor that creates the contrasts and allows the detection of organic contamination by GPR. Reflections from the interstitial hydrocarbon are function of the permitivity contrast between the hydrocarbon and the "host" material. Actually, a detectable contrast is dependent on the relative contrasts between the different soil composition and the liquid present at the interface. Usually LNAPLs values are low and do not give an appreciable contrast with sand or gravel. Otherwise, it may give a good contrast with clayey soil.

The conceptual geoelectric model of hydrocarbon contamination plumes considers the plume as a resistive material since these substances are apolar. On the other hand, field and laboratory studies have shown that the plume can acquire conductive behavior with the time due to biodegradation process (Sauck et al., 1998; Werkema et al., 2000; Cassidy et al., 2001).

The GPR technology is relatively recent but the data processing has been intensively studied since both the processing techniques and software from the seismic method can be applied considering the cinematic aspect. It can be observed in the GPR literature that the technical language of the seismic is applied as well as the acquisition and data processing terminology. The possibility to apply the same techniques from the reflection seismic is presented in several works (Szaraniec, 1979; Ursin, 1983; Lee et al., 1987). Fisher et al. (1992, 1994 and 1996) applied seismic processing techniques to GPR data and had good results.

The GPR field data presents a) reflections, b) coherent noise, c) environment noise and, eventually, d) instrument noise. An important aspect of the data processing is to discriminate the real data (reflections) from the several types of noise.

METHODOLOGY

In order to carry out the research, a typical urban problem was selected with the Environmental Agency of São Paulo (CETESB) and covered the steps as follows:

1.gathering of the geological, hydrogeological data and the contamination process history;
2.definition of the location of the GPR profiles in order to map the contamination plume;
3.execution of a GPR "noise analysis", sounding of several GPR sections and a CMP sounding to define the propagation velocities in the contaminated and non-contaminated sediments and the acquisition parameters;
4.visual interpretation of the processed GPR sections;
5.development of tools trying to minimize the interpret judgment;
6.based on the preceding items, auger boreholes were made to evaluate the properness of the premises adopted.

Case Study

Geology

The study area (Figure 1) is located over Quaternary alluvial deposits (sand-clayey) associated with the Tiete River. Locally, the gas station is over a heterogeneous landfill (varying from 2.5 to 4.5 ft thick) overlaying a plastic clay layer of 3.6 to7.2 ft thick.

Figure 1 – Location of the study area, in the city of São Paulo (Brazil).

Hydrogeology

The hydrogeological context is dominated by two distinct systems, presenting characteristics of porous and fractured aquifers. In the gas station site, based on sampling and measurements carried out in the boreholes, the sediments are predominantly clayey and the water level varied from 4.6 to 7.5 ft of depth in 1997 and between 2.2 and 6.9 ft in 2001. An extremely low gradient allows the frequent inversion of the groundwater flow.

Contamination Characteristics

The contamination was firstly observed in 1997 and several monitoring and remediation boreholes were installed. This allowed monitoring of the groundwater level variation and the evolution of the contaminant plume. The remediation was based on the pumping and treating process of the free phase.

During the first GPR research (July 2000) a very thin free phase layer was observed in few boreholes. After the second GPR research (January, 2000), another inspection was performed in the area, jointly with CETESB, when measurements of the level and conductivity of the groundwater, thickness of the free phase, and observation of the water appearance and smell were taken. In addition, during the boring and sampling performed for verification in January 2001, volatile smell was noted from the soil and groundwater samples of the F4, F6 and F7 boreholes (Figure 2).

The GPR used was a RAMAC (Mala – Geoscience) with conventional antennae of 100 and 200 MHz and a 250MHz shielded antennae. The RAMAC2 (v. 2.28 – 1997) acquisition software and RADPRO (v. 2.25 – 1996) processing software were used.

Previous studies indicated a contamination plume as presented in Figure 2. The data acquired in the study area consisted of a series of GPR sections during two phases (July, 2000 and January, 2001) of surveying as also presented in Figure 2.

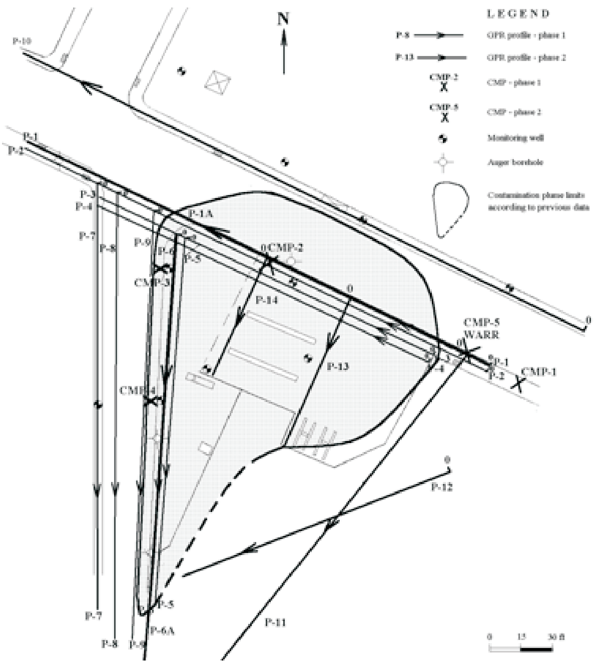

Figure 2 – Study area map lines showing contamination plume according to visual interpretation of GPR data and location of the survey.

Instrumentation

During the first phase 9 GPR sections (P1 to P9) with total extension of 1919 ft were carried out. A common offset, single-fold array was adopted and the station spacing was 0.33 ft, resulting 5,830 traces. The 250 MHz shielded antennae was used. In addition, four CMP (commom middle point) soundings were performed over the section P1 using antennae of 100 and 200 MHz. The first two (CMP1_100 and CMP1_200) on an area with no contamination indication while the last two (CMP2_100 and CMP2_200) on a contaminated area. In all cases the stacking was 128.

In the second phase the sections P1 and P6 were repeated and five new sections were sounded (P10 to P14). Three new CMP soundings (CMP3, CMP4 and CMP5) and one WARR (wide angle reflection and refraction) coincident with CMP5, were carried out. The total extension was 3063 ft, with 8,690 traces. In this phase the 128 and 256 stacking were tested.

Data Processing

The data processing began with a spectral analysis followed by the application of a DC filter, AGC and final filter. For the 100 MHz acquisition it was also applied a deconvolution step.

After the processing it was observed indications that could be associated with the contamination. A typical shadow zone, as related by Nash et al. (1997), Bermejo et al. (1997), Aquino et al. (1998), Orlando (2002), was considered as being the contaminated area. The sections were then divided into zones where the indication of contamination was present and zones with no contamination indication. After that, a new spectral analysis was carried out to evaluate the energy distribution between different groups of traces and between different time periods. The spectral analysis was divided into three different time periods (0 to 30 ns, 30 to 60 ns and 60 to 100 ns) since the contamination was associated with a shadow zone between 30 and 60 ns, very evident in four of the sections (P1, P6, P13 and P14). The sections P7, P8 and P9 were considered as "background" because no shadow indication was observed while P10, P11 and P12 presented a subtle and dubious indication.

The spectral analysis was performed in three steps: 1) considering all traces; 2) considering only the traces where the shadow zone was observed and 3) considering only the traces without evidence of shadow zone. The results (of one of the sections) are presented in Figures 4, 5 and 6.

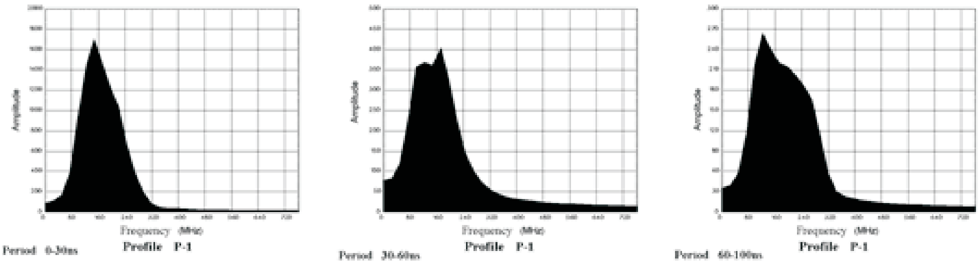

Figure 3 – Spectral analysis considering all traces

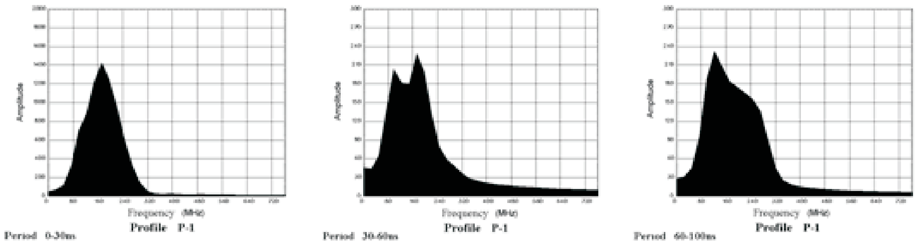

Figure 4 – Spectral analysis considering only traces where the shadow zone was observed

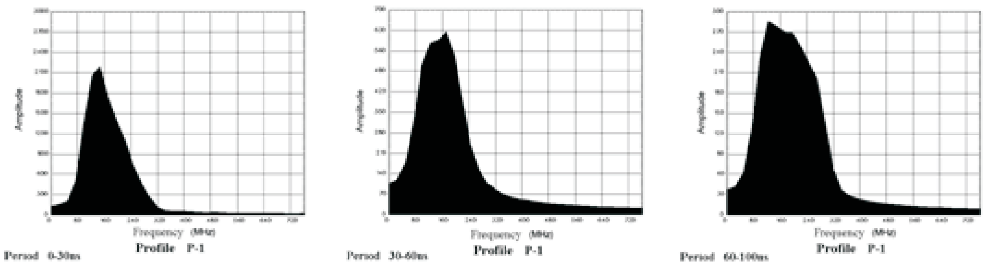

Figure 5 – Spectral analysis considering only traces without evidence of the shadow zone

Spectral Analyses

The graphs show that on the contaminated area the highest amplitude frequency maintains the energy in the last two time periods (30-60 ns and 60-100 ns). On the other hand, the same comparison for the non-contaminated area shows a decreasing energy content in the last time period (60-100 ns), similar to the behavior to the full section analysis.

The spectral analyses carried out to compare the signal behavior in both spatial and time series show that the signal energy content does not present significant change in the regions where the shadow zone appeared.

The uniform energy content until the end of the section in the contaminated zones occurs probably due to homogenization caused by the hydrocarbon presence and, consequently, the signal propagates without reflections. In this case there is no energy loss since the signal is not reflected to the surface and the medium acquires higher resistivity due to the hydrocarbon presence, which occupies the porous space of the material in substitution of the water.

The qualitative visual analyses performed initially led to good results that could be confirmed by the spectral results.

In order to diminish the subjective analyses, a calculation of the amplitude ratio (AR) was performed. The amplitude ratio is the ratio between the maximum spectrum amplitude obtained in the shadow zone (APS) and the maximum amplitude of the total section (ATS).

$$AR = \frac{A_{ts}}{A_{ps}}$$

APS was measured on the time period that presented shadow zone (30 to 60 ns) for each 1/10 of the total section traces. ATS is the spectral amplitude of the total section in both time and distance. The AR values were plotted in the medium point of the 1/10 of the traces considered.

The spectra show that the APS related to the shadow zone are smaller than the respective ATS. Therefore, AR values greater than 1 (AR>1) should be related to the shadow zone. It is important to observe that if the shadow zone is present in all the section (p.e. sections P-13 and P-14) the AR value is smaller than that of a section where the shadow zone is present only in a part of it. This means that greater AR values are not necessarily related to a larger contaminated zone. For that reason, it is important that the survey reaches zones without contamination, in order to allow a background value that differentiates the ATS from APS spectra.

Geostatistical Analysis

In order to determine the spatial correlation of AR and APS variables, semivariograms were computed along four main directions. As long as the computed semivariograms did not show some anisotropy, an omnidirectional semivariogram was considered.

In a previous semivariogram analysis, it was concluded that both AR and APS variables do not present some anisotropy. Therefore, the spatial correlations for these variables were determined using omnidirectional experimental semivariograms, to which spherical models were fitted according to Figures 6 and 7.

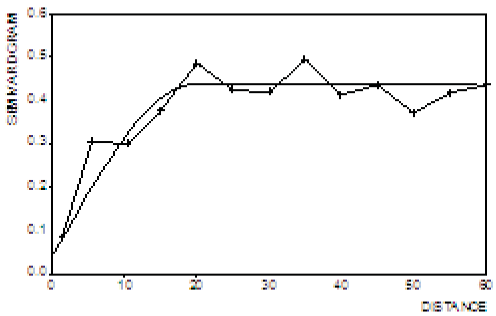

Figure 6 - Semivariogram model for AR variable - range is 65.6 ft (20 m).

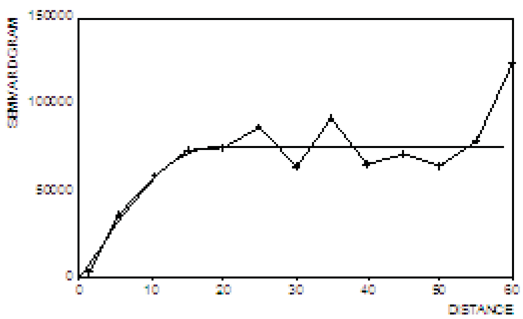

Figure 7 - Semivariogram model for APS variable - range is 59.0 ft (18 m).

Both semivariogram models show a zone of influence around 59-66 ft, as indicated by their respective ranges. It means that the contamination zone spreads approximately 65 ft from its source, which is observed also by the hydrochemical analyses.

Thus, spatial distribution of RA and APS variables were drawn based on ordinary kriging estimates according to Figures 9 and 10, respectively.

In Figure 9 values greater than 1 are related to the contamination and the interpolation of the calculated AR values allowed delineating the contamination plume.

Figure 10 shows the spatial distribution of APS. In this case the smaller values are related to the shadow zone. The maximum APS value used to limit the contamination plume was 400 since this was the minimum ATS value observed in the background sections (p.e. P-10). Therefore, it may be considered that the contamination plume is mainly concentrated in the region with values equal to or smaller than 400.

The comparison of the contamination plume presented in Figure 2 with those presented in Figures 9, 10 and 11 shows that the four maps are similar but, in the first, the plume is limited by the avenue, while in the other three maps the plume reaches the section P-10.

In order to check the properness of the numerical analysis, an auger borehole was performed in that point (PMAdc-1) and both free and dissolved phases of the hydrocarbon were observed. This fact confirms that the criterium used is efficient and has a good correlation with the subsurface contamination area.

FINAL DISCUSSION

The presence of hydrocarbon in the subsurface modifies the medium. As the hydrocarbon (vapor and liquid phases – K=2) occupies the porous space, part of the water (K=80) is replaced and this certainly changes the natural situation, particularly the dielectric constant that the medium had before the contamination process.

The anomaly related to the contamination is characterized by the lack of signal and has been called as "shadow zone" and that could be observed in the study area through monitoring wells.

The use of shielded antennae in a highly urbanized area was fundamental in this research and must always be considered in gas station related contamination problems, despite the impossibility to carry out CMP or WARR profiles with such antennae.

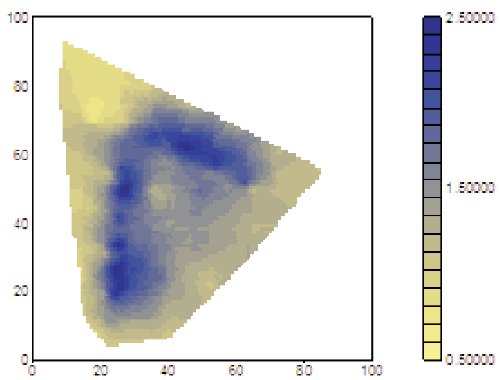

Figure 8: Spatial distribution for AR variable based on ordinary kriging estimates.

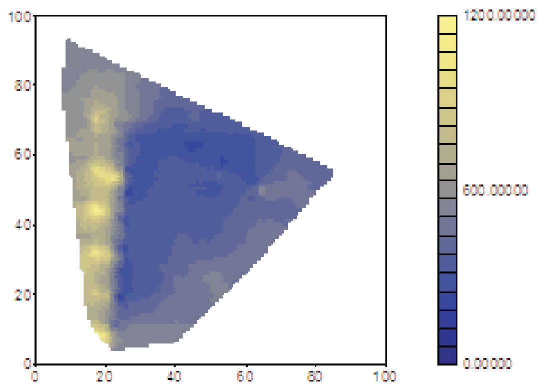

Figure 9: Spatial distribution for APS variable based on ordinary kriging estimates

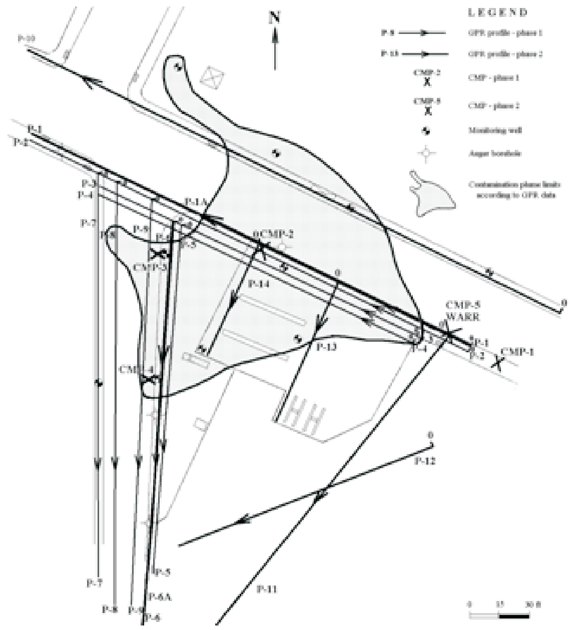

Figure 10 – Final delineation of the contamination plume based on the numerical treatment of the GPR data and auger borehole.

The use of stacking greater than 128 allowed a broader shadow zone but it was not clear, in this research, if this total area was contaminated. Therefore stacking greater than 128 must be carefully considered since the acquisition time is a direct function of the stacking adopted.

The velocity analysis confirms that the contaminated area presents lower dielectric constant values (P-13 and P-14) than the background (P-7, P-10 and CMP-1). The signal propagation velocity is higher in the sections that presented shadow zone, due to the lower dielectric constant. Even for the section P-7, carried out during the dry season the dielectric constant was higher, which shows that the radar signal in a contaminated area is different than the signal of an area with lower water content.

The spectral analyses carried out with the contaminated portions (both spatial and temporal) confirm that the shadow zone in this case is due to the lack of reflection because the energy content stays practically the same in the next period (60 to 100 ns) of the corresponding shadow zone (30 to 60 ns). This behavior is different than the observed in the non-contaminated area where the energy is attenuated with the depth (with the time). In the study area the anomaly related to the contamination appears as lack of signal in the processed sections. The most important observations were obtained through auger boreholes, soil sampling and analyses, which showed that the shadow zone was effectively related to the contamination.

The extent of the contamination plume as obtained by the radar data interpretation allowed concluding that it was larger than firstly estimated by the chemical analyses.

ACKNOWLEDGEMENTS

The authors express their gratitude to the Conselho Nacional de Desenvolvimento Científico e Tecnológico (CNPq) for the scholarship of the senior author.

REFERENCES

1.AQUINO, W.F.; DEHAINI, J.; MENDES, J.M.B. (1998) Geo-Radar para detecção de contaminação por hidrocarboneto. Anais do II Workshop de Geofísica Aplicada. Rio Claro, SP. (CD-ROM)

2.BENSON, A.K. (1995) Applications of ground penetrating radar in assessing some geological hazards: examples of groundwater contamination, faults, cavities. Journal of Applied Geophysics. Elsevier Science B.V., Amsterdam. v 33. p 177-193.

3.BENSON, A.K.; PAYNE, K.L.; STUBBEN, M.A. (1997) Mapping groundwater contamination using dc resistivity and VLF geophysical methods - A case study. Geophysics, v 62, n 1, p 80-86.

4.BERMEJO, J. L.; SAUCK, W. A.; ATEKWANA, E. A. (1997) Geophysical discovery of a new LNAPL plume at the Former Wurtsmith AFB, Oscoda, Michigan. Ground-Water Monitoring Review. Fall, p 131-137.

5.DANIELS, J.J.; ROBERTS, R.; VENDL, M. (1995) Ground penetrating radar for the detection of liquid contaminants. Journal of Applied Geophysics. Elsevier Science B.V., Amsterdam. v 33. p 195-207.

6.DAVIS, J.L. & ANNAN, A.P. (1989) Ground-penetrating radar for high resolution mapping of soil and rock stratigraphy. Geophysical Prospecting, v 37, p. 531-551.

7.DEHAINI, J. (2001) Detecção da pluma de contaminação de hidrocarbonetos em subsuperfície pelo método de radar de penetração. Tese de Doutoramento. Instituto de Geociências da Universidade de São Paulo. 100p.

8.FISHER, E; McMECHAN, G.A.; ANNAN, A.P. (1992) Acquisition and processing of wide-aperture ground-penetrating radar data. Geophysics. v. 57, n. 3, p 495-504

9.FISHER, S.C.; STEWART, R.R.; JOL H.M. (1994) Processing ground penetrating radar data. Proceedings of the Fifth International Conference on Ground Penetrating Radar. p 661-675

10.FISHER, S.C.; STEWART, R.R.; JOL H.M. (1996) Ground penetrating radar (GPR) data enhancement using seismic techniques. Journal of environmental and engineering geophysics. v. 1, n. 2, p 89-96.

11.HIDROPLAN - Hidrogeologia e Planejamento Ambiental S/C Ltda (1997) Laudo técnico de avaliação sobre a situação de contaminação em área próxima ao Auto Posto na Freguesia do Ó, São Paulo, SP. (Restricted).

12.KELLER, G.V. & FRISCHKNECHT, F.C. (1966) Electrical methods in geophysical prospecting. Pergamon press Inc. N.Y. 519p.

13.LEE, S; McMECHAN, G.A.; AIKEN, C.L.V. (1987) Phase-field imaging: The electromagnetic equivalent of seismic migration. Geophysics, v 52, n 5, p 678-693.

14.LANE Jr., J.W.; BUURSINK, M.L.; HAENI, F.P.; VERSTEEG, R.J. (2000) Evaluation of Ground-Penetrating Radar to Detect Free-Phase Hydrocarbons in Fractured Rocks – Results of Numerical Modeling and Physical Experiments. Ground Water, v. 38, no 6, pg 929-938.

15.NASH, M.S.; ATEKWANA, E.; SAUCK, W.A. (1997) Geophysical investigation of anomalous conductivity at a hydrocarbon contaminated site. Proceedings of the Symposium on the Application of Geophysics to Engineering and Environmental Problems (SAGEEP). v 2, p 675-683.

16.NGUYEN,V.T.; QUICK,M.J.; ERIKSEN,A.S.; BOOTH,S.; ROEST,D.; WAGEBERT,A.; Al-NUAMY,W.; NAKHKASH,M.; ZHANG,D.;HUANG, Y. (1997) An evaluation of geophysical techniques to measure sub-surface hydrocarbon contamination at a disused fuel distribution depot. Proceedings of the Symposium on the Application of Geophysics to Engineering and Environmental Problems (SAGEEP), v 1, p. 251-259.

17.ORELLANA, E. (1982) Prospeccion geoelectrica en corriente continua. Madrid, Ed. Paraninfo. 578p.

18.ORLANDO, L. (2002) Detection and analysis of LNAPL using the instantaneous amplitude and frequency of ground-penetrating radar data. Geophysical Prospecting, n.50, p. 27-41.

19.RADPRO (1996) Data processing manual - GPR RAMAC version 2.25. Malä-Geoscience. 52p.

20.RAMAC/GPR (1997) Instrument Manual version 2.28. Malä-Geoscience. 65p

21.SAUCK, W.A., ATEKWANA, E.A., NASH, M.S. (1998) High conductivities associated with an LNAPL plume imaged by integrated geophysical techniques. Journal of Environmental and Engineering Geophysics. v 2, n 3, p 203-212.

22.SZARANIEC, E. (1979) Towards unification of geophysical problems for horizontally stratified media. Geophysical prospecting, v 27, n 3, p 576-583

23.TELFORD, W.M.; GELDART, L.P.; SHERRIF, R.E. (1990) Applied geophysics. Cambridge, Cambridge University Press. 770p

24.TOPP,G.C.; DAVIS,J.L.; ANNAN, A.P. (1980) Eletromagnetic determination of soil water content: measurements in coaxial transmission lines. Water Resources Research. v 16, n 3, p 574-582

25.URSIN, B. (1983) Review of elastic and electromagnetic wave propagation in horizontally layered media.

Geophysics, v 48, n 8, p 1063-1081.
26.WERKEMA, Jr., D.D.; ATEKWANA, E.; SAUCK, E; ROSSBACH, S.; DURIS, J. (2000) Vertical distribuition of microbial abundances and apparent resistivity at an LNAPL spill site. Proceedings of the Symposium on the Application of Geophysics to Engineering and Environmental Problems (SAGEEP), p 669-678